Journal of Hazardous Materials 283 (2015) 730–739

Contents lists available at ScienceDirect

Journal of Hazardous Materials

journal homepage: www.elsevier.com/locate/jhazmat

Polydopamine-coated electrospun poly(vinyl alcohol)/poly(acrylic acid) membranes as efficient dye adsorbent with good recyclability

Jiajie Yan[a], Yunpeng Huang[a], Yue-E Miao[a], Weng Weei Tjiu[b], Tianxi Liu[a,*]

[a] State Key Laboratory of Molecular Engineering of Polymers, Department of Macromolecular Science, Fudan University, Shanghai 200433, PR China
[b] Institute of Materials Research and Engineering, A*STAR (Agency for Science, Technology and Research), 3 Research Link, 117602, Singapore

HIGHLIGHTS

- Polydopamine coated electrospun PVA/PAA membrane was prepared as a novel adsorbent.
- The PVA/PAA@PDA membrane can adsorb more than 93% of methyl blue within 30 min.
- The maximum adsorption capacity of adsorbent for methyl blue is 1147.6 mg g^{-1}.
- The PVA/PAA@PDA membrane shows good performance on adsorbing various dyes.
- The membrane adsorbent is easy to operate and possesses good recyclability.

GRAPHICAL ABSTRACT

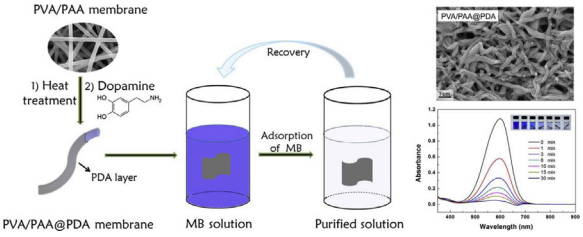

Free-standing poly(vinyl alcohol)/poly(acrylic acid) membranes with polydopamine coating (PVA/PAA@PDA) were prepared based on the combination of electrospinning and self-polymerization of dopamine. Benefiting from the high specific surface area of electrospun membranes and the abundant "adhesive" functional groups of polydopamine, the as-prepared membranes exhibit efficient adsorption performance toward methyl blue with the maximum adsorption capacity reaching up to 1147.6 mg g^{-1}. Moreover, compared to other nanoparticle adsorbents, the as-prepared self-standing membrane is highly flexible, easy to operate and retrieve, and most importantly, easy to elute and regenerate, which enable its potential applications in wastewater treatment.

ARTICLE INFO

Article history:
Received 9 June 2014
Received in revised form 17 October 2014
Accepted 26 October 2014
Available online 31 October 2014

Keywords:
Electrospinning
Polydopamine
Adsorption
Methyl blue

ABSTRACT

Free-standing poly(vinyl alcohol)/poly(acrylic acid) (PVA/PAA) membranes with polydopamine (PDA) coating were prepared based on the combination of electrospinning and self-polymerization of dopamine. This is a facile, mild, controllable, and low-energy consumption process without any rigorous restriction to reactive conditions. Benefiting from the high specific surface area of electrospun membranes and the abundant "adhesive" functional groups of polydopamine, the as-prepared membranes exhibit efficient adsorption performance towards methyl blue with the adsorption capacity reaching up to 1147.6 mg g^{-1}. Moreover, compared to other nanoparticle adsorbents, the as-prepared self-standing membrane is highly flexible, easy to operate and retrieve, and most importantly, easy to elute, and regenerate, which enable its potential applications in wastewater treatment.

1. Introduction

The rise of manufacturing industry from last century brings a period of growth and prosperity to many countries, but also causes kinds of pollution problems. Among various pollutions, water contamination with organic dyes released by related industries attracts widespread attention due to their adverse effects on the

* Corresponding author. Tel.: +86 21 55664197; fax: +86 21 65640293.
E-mail address: txliu@fudan.edu.cn (T. Liu).

http://dx.doi.org/10.1016/j.jhazmat.2014.10.040
0304-3894/

environment and public health [1,2]. Therefore, the removal of dye wastes is becoming an urgent issue to study and press forward. To date, lots of approaches have been reported to remove dyes from wastewater, e.g., biological treatment [3], chemical technologies (e.g., ion-exchange [4], oxidation [5], and photocatalytic degradation [6]), and physical methods (e.g., adsorption and membrane filtration [7]). Among these techniques, adsorption proves to be one of the most attractive solutions because of its relatively high efficiency, simple design, convenient operation, and no secondary pollution [8–10]. However, many traditional adsorbents, for instance, activated carbon [11], clays [12,13], silica [14], chitosan [15,16], and polymer resins [17,18], suffer from the limitation of adsorption capacity, efficiency, and recycling ability. Therefore, it is of great importance for the development of efficient dye waste adsorbents with large adsorption capacity, good flexibility, and recyclability.

Electrospinning is a promising method for producing continuous fibers with diameters ranging from tens of nanometers to several micrometers [19]. The obtained fibrous membranes exhibit many outstanding characteristics such as high porosity, large surface area to volume ratio, and excellent flexibility, making them ideal candidates for catalysts, sensors, drug carriers, and protective clothing, as well as in ultrafiltration, and separation applications [20–22]. In recent years, electrospun membranes equipped with specific functional groups have attracted increasing interests for their potential applications in contaminant adsorption [23,24]. Zhang et al. have employed chitosan as a modifier and Cibacron Blue F3GA as a ligand tethered onto electrospun polyacrylonitrile surface to form a dual-layer biomimetic membrane, which exhibits an excellent capturing ability for bromelain [25]. Miao et al. have combined electrospinning and hydrothermal reaction to prepare hierarchical SiO_2@γ-AlOOH (Boehmite) core/shell fibers for water remediation [26]. It is obvious that electrospun membranes can successfully meet the increasingly challenging standards for applications in wastewater treatment fields.

Inspired by the properties of adhesive proteins in marine mussels, dopamine, which belongs to a class of catecholamines, was able to self-polymerize under basic reaction conditions and form a polydopamine (PDA) film onto almost all types of substrates [27,28]. The PDA coating can generate a highly stable polymer layer on the surface of the target and shows special adhesive ability in the presence of residual catechol groups on the PDA layer, which facilitates further reactions with proper molecules and opens up the possibility of tailoring the PDA coating for various applications [29]. For instance, the PDA film has often been employed as a modifier to improve the hydrophilicity and reactivity of aimed substrates, such as clay [30], polystyrene nanofibers [31], and even polytetrafluoroethene [32]. In particular, Gao et al. have prepared PDA functionalized graphene hydrogel via a one-step method and found that the PDA-coated graphene hydrogel showed good adsorption capacity for heavy metal and organic dye in wastewater [33]. And recently, the PDA decorated nanoparticles (e.g., Fe_3O_4 [34] and natural zeolites [35]) have also been synthesized and applied for removal of multiple pollutants. However, considering the environmental issue mentioned above, more studies should be explored by focusing on the usage of polydopamine as adsorbent for dye pollutants removal from water.

Herein, to address the challenge, we successfully developed a free-standing electrospun poly(vinyl alcohol)/poly(acrylic acid) (PVA/PAA) membrane functionalized with PDA as an adsorbent for organic dyes. A typical PVA/PAA blend system was selected as the appropriate material for electrospinning due to its good water-stability and mechanical properties [36]. After polymerization of functional PDA layer on the surface of PVA/PAA nanofibers, the adsorption performance of the membranes towards methyl blue has been significantly improved. In addition, the adsorbent in flexible membrane form can be easily retrieved from the dye solution and regenerated by NaOH for multiple cycles, which further broadens its potential applications in dye adsorption.

2. Experimental

2.1. Materials

PVA (Mw from 85 000 to 124 000, 98–99% hydrolyzed) was purchased from Sigma–Aldrich. PAA (Mw ≈ 1800, 25 wt% aqueous solution) and hydroxyphenethylamine hydrochloride (dopamine, 98%) were obtained from Aladdin Chemical Reagent. Tris(hydroxymethyl) aminomethane (TRIS, 99%) and tris(hydroxylmethyl) aminomethane hydrochloride (Tris–HCl, 99%), which were used as buffer agents, were purchased from Alfa Aesar. Methyl blue (MB) and NaOH were supplied by Sinopharm Chemical Reagent Co., Ltd. Deionized water was used as solvent for all experiments. All other reagents were of analytical grade and used without further purification.

2.2. Preparation of electrospun PVA/PAA nanofiber membranes

PVA was dissolved in deionized water under magnetic stirring at 80 °C for 12 h to prepare a 10 wt% aqueous solution. The PAA solution was diluted to a concentration of 12 wt%, and stirred at room temperature for 1 h. Then, the as-prepared PVA and PAA solutions were mixed with a volume ratio of 1:1 [37]. The resulting mixture was further stirred at room temperature for 1 h to obtain a homogeneous solution for electrospinning.

5 mL of PVA/PAA mixture was loaded into a syringe connected to a stainless steel needle with an inner diameter of 0.5 mm. A voltage of 15 kV and a feeding rate of 0.5 mL h^{-1} was applied to the spinneret. The electrospun nanofiber membranes were carefully detached from an aluminum collector, which was placed 20 cm away from the needle, and then dried in vacuum at room temperature for 24 h. After that, the temperature was raised and maintained at 120 °C for 3 h for heat-induced crosslinking reaction between PVA and PAA.

2.3. Preparation of PDA-coated PVA/PAA (PVA/PAA@PDA) membranes

The PVA/PAA@PDA membranes were prepared according to the literature [33]. After crosslinking at 120 °C, PVA/PAA membranes became insoluble in water which was induced by the esterification reaction between the carboxylic acid groups of PAA and hydroxyl groups of PVA [37]. Then the membranes were immersed into an aqueous solution of dopamine (2 mg mL^{-1} in 10 mM Tris buffer, pH 8.5) with mild stirring at 50 °C for PDA coating. And the as-prepared membranes were named as PVA/PAA@PDA-5, PVA/PAA@PDA-15, PVA/PAA@PDA-30, and PVA/PAA@PDA-45 according to the reaction time (5 h, 15 h, 30 h, and 45 h, respectively). After the reaction, the membranes were thoroughly washed with deionized water and ethanol for several times to remove the non-adhered PDA, and dried in a vacuum oven at 80 °C for 24 h.

2.4. Adsorption experiments

For the adsorption experiments, an aqueous solution of MB was chosen as the model contaminant. A certain amount of PVA/PAA@PDA membranes (10–12 mg) was added into MB solution (50 mL) under a magnetic stirring of 160 rpm at room temperature. At each time interval, 1 mL of the solution was withdrawn and diluted to the proper concentration, which was measured by UV spectrophotometer at 600 nm. The adsorbed

amount of MB on the adsorbent was calculated using the following equation:

$$q_t = \frac{(C_o - C_t)V}{m} \quad (1)$$

where q_t (mg g^{-1}) is the absorption amount of MB at time t; C_o (mg L^{-1}) and C_t (mg L^{-1}) are the initial concentration of MB and the concentration at time t, respectively; V (L) is the volume of the solution and m (g) is the mass of the membrane.

For the study of adsorption isotherms, MB solution (50 mL) with different concentrations (i.e., 50, 100, 200, 400, 800, and 1000 mg L^{-1}) was mixed with PDA coated membranes (10–12 mg) for certain time. The following equation was used for the calculation of absorbed amount of MB at equilibrium:

$$q_e = \frac{(C_o - C_e)V}{m} \quad (2)$$

where q_e (mg g^{-1}) and C_e (mg L^{-1}) are the equilibrium adsorbed amount and concentration of MB, respectively.

For the recycling experiments, the as-prepared PVA/PAA@PDA membranes (10–12 mg) were added into 50 mL of MB solution (100 mg L^{-1}) under stirring at 160 rpm. After 3 h of adsorption, the membranes were transferred into NaOH solution (0.5 mol L^{-1}) for 10 min to elute the adsorbed matters. After elution, the membranes were rinsed with deionized water and ethanol for several times until the washing solution reaches neutral to remove any trace of NaOH. The adsorption-desorption processes were repeated for ten times using the same membrane, initial MB concentration, and NaOH solution. Schematic illustration of the whole process for preparation of PVA/PAA@PDA membrane and its application for dye adsorption was presented in Fig. 1.

2.5. Characterization

The morphology of the membranes was observed by field-emission scanning electron microscope (FESEM, Ultra 55, Zeiss). The chemical composition of the samples was examined by X-ray photoelectron spectroscopy (XPS) with a VG ESCALAB 220I-XL device. All XPS spectra were corrected according to the C1s line at 285.0 eV. Curve fitting and background subtraction were accomplished using Casa XPS software. The concentrations of MB solution were calibrated and determined by UV–vis spectrophotometer (PerkinElmer, Lambda 35) at the wavelength of 600 nm.

3. Results and discussion

3.1. Morphology and structure of PVA/PAA@PDA membranes

In this work, we combine the advantages of electrospun nanofiber membranes and polydopamine by introducing PDA coating onto the surfaces of electrospun nanofibers. PVA/PAA nanofiber membranes were prepared through electrospinning method, followed by thermal crosslinking treatment to render them water-stable. And the PDA layer was obtained via the self-polymerization of dopamine in mild aqueous conditions. In simple terms, the amine and catechol groups on dopamine can be covalently conjugated via the quinone groups, and the final formation of PDA is similar to the formation of melanin in the skin [38]. In the present study, we focused on the exploration of the adsorption performance of PVA/PAA@PDA membranes towards a common dye, methyl blue.

After heat treatment, the original white membrane (Fig. S1(a)) turned into pale yellow (Fig. S1(b)) as a result of the crosslinking between carboxylic acid groups of PAA and hydroxyl groups of PVA [32]. Moreover, a significant color change was found for the membranes after PDA coating (Fig. S1(c–f)). The black color of PDA-coated PVA/PAA membranes was resulted from the self-polymerization of dopamine onto the surface of PVA/PAA nanofibers. It is obvious that with the increase of PDA loading, the color of membranes gradually changes from pale yellow to dark brown, and finally turned to black. Besides, for the original PVA/PAA, crosslinked PVA/PAA, PVA/PAA@PDA-5, and PVA/PAA@PDA-15 membranes, no crack appeared after bending and flattening for several times, indicating high flexibility of the membranes (Fig. S1(g)). However, same performance was not observed for PVA/PAA@PDA-30 and PVA/PAA@PDA-45 membranes. The morphologies of the membranes were observed by FESEM (Fig. 2). For the original PVA/PAA membrane, the nanofibers show smooth surface and uniform morphology with a narrow fiber diameter distribution (200–300 nm). After heat-treatment at 120 °C for 3 h, inter-adhesions of electrospun nanofibers were observed because of the esterification reaction between PVA and PAA (Fig. 2b). Furthermore, upon increasing the immersion time, the PDA layer first varied from thin (PVA/PAA@PDA-5, Fig. 2c) to thick (PVA/PAA@PDA-15, Fig. 2d). Then, small PDA particles were formed and appeared on the fiber surface (PVA/PAA@PDA-30, Fig. 2e). Further increasing the reaction time, redundant PDA particles stacked or agglomerated between the fibers, thus blocked the porous structure of PVA/PAA@PDA-45 nanofiber membranes (Fig. 2f). It can be deduced that the increased thickness of the

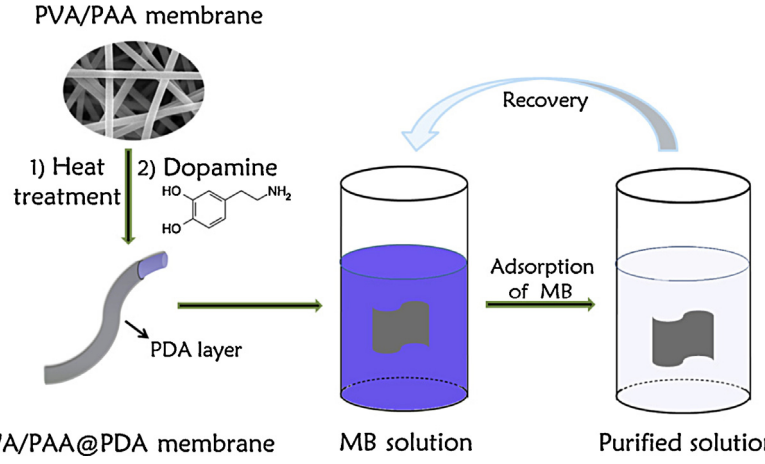

Fig. 1. Schematic illustration of the preparation of PVA/PAA@PDA membranes and their applications for dye adsorption.

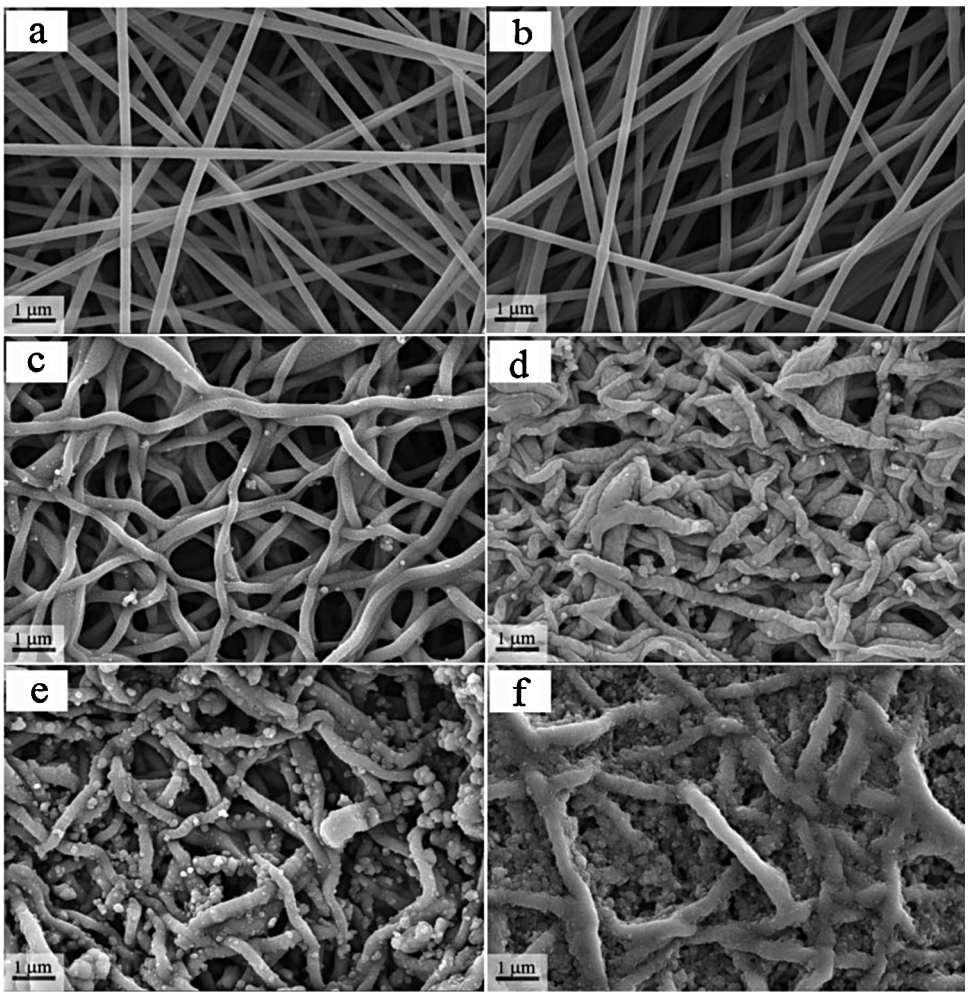

Fig. 2. FESEM images of original PVA/PAA membrane (a), PVA/PAA membrane after heat treatment (b), PVA/PAA@PDA-5 (c), PVA/PAA@PDA-15 (d), PVA/PAA@PDA-30 (e), and PVA/PAA@PDA-45 (f) membranes.

PDA coating and PDA aggregation may be responsible for the deterioration of the mechanical properties for the PVA/PAA@PDA membranes.

The surface chemical compositions of PVA/PAA membranes before and after PDA coating were analyzed using XPS, as shown in Fig. 3. The peaks of O 1 s and C 1 s are both observed in PVA/PAA and PVA/PAA@PDA membranes, while a considerable difference was revealed in PVA/PAA@PDA membrane with the high resolution nitrogen peak (N 1 s, 400.3 eV), which should arise from the PDA layer on the surface, consistent with previous reports [35,39,40]. Moreover, the C 1 s core-level spectrum of the two membranes was further investigated. For PVA/PAA membrane, the C 1 s signal can be curve-fitted with three peak components at the binding energies of about 285, 286.4, and 289.2 eV, attributable to the C—C/C—H, C—O, and O—C=O species, respectively (Fig. 3C). After PDA coating, the C 1 s spectrum of PVA/PAA@PDA membrane also shows the presence of C—N species (at 286.2 eV), and this peak associated with C—C/C—H becomes dominant (Fig. 3D). Collectively, these results strongly suggest that PDA was successfully coated on PVA/PAA fibers.

3.2. Adsorption performance of PVA/PAA@PDA membranes and the adsorption mechanism

PVA/PAA@PDA membranes were used as adsorbent for potential applications in water purification because of its porous structure and the adhesive property derived from PDA coating. MB, a common dye in textile industry, was selected as the target pollutant in our experiments. As shown in Fig. 4A, the absorption peaks decrease significantly within 30 min, indicating an efficient adsorption of the PVA/PAA@PDA membrane towards MB. The insets of Fig. 4A are the digital photographs of MB solutions after treatment at the corresponding given time intervals. It can be seen that the color of MB solution varied from dark blue to light blue within 10 min, and nearly colorless after 30 min, which provides a visible track for the efficient adsorption of the membrane adsorbent. Moreover, as presented in Fig. 4B, the quantitative results indicate that more than 93% of MB in solution can be adsorbed in a short time (30 min) when the PVA/PAA@PDA membrane is used as an adsorbent.

According to previous study [35], the highly effective adsorption of PVA/PAA@PDA membrane towards MB may be attributed to the electrostatic interaction and hydrogen bonding between the negatively charged oxygen functional groups present on the surface of PDA and the amine groups of MB. Because the surface charge of the adsorbent as well as the degree of ionization of MB is affected by pH, it's necessary to study the influence of pH on the adsorption of MB. A series of equilibrium adsorption experiments have been carried out at various pH values as shown in Fig. 5. The pH values of the solution are adjusted by addition of 1 M NaOH and 1 M HCl. It can be seen that the dye uptake was higher at lower pH and as the pH of the solution increased, dye uptake decreased considerably. The results may be attributed to the following factors. At acidic pH, the adsorbate possesses positive charge because

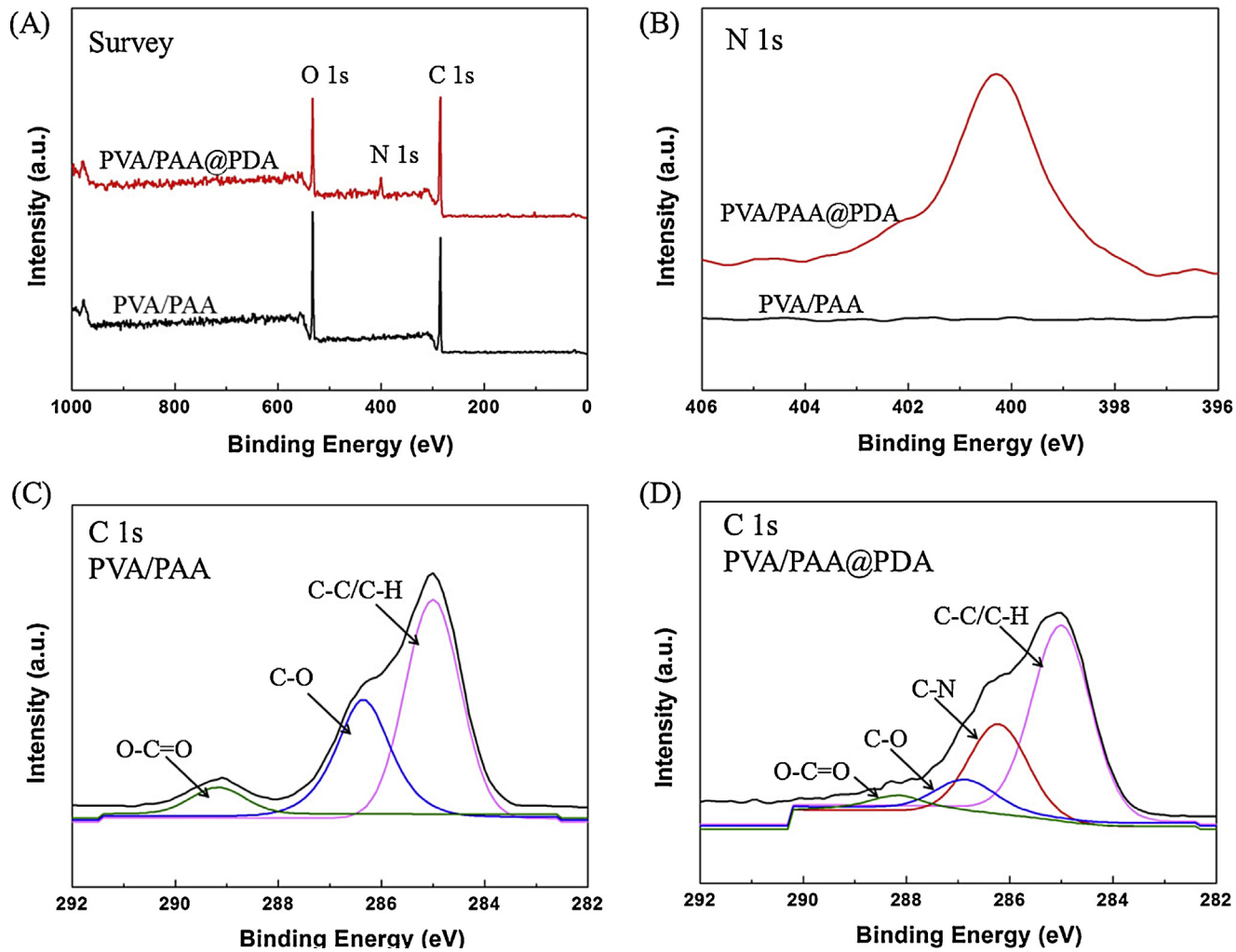

Fig. 3. XPS survey spectra of PVA/PAA and PVA/PAA@PDA-15 membranes (A), high-resolution XPS spectra of N 1 s peaks for PVA/PAA and PVA/PAA@PDA-15 membranes (B). High-resolution XPS spectra of C 1 s peaks for PVA/PAA (C) and PVA/PAA@PDA-15 (D) membranes.

the amino groups of MB were protonated to form amino cations, while the adsorbent species are still negatively charged. And with the pH decreasing, more and more amino cations formed, so the adsorbent can adsorb more quantity of anionic dye at lower pH. In contrast, the lower sorption uptake at higher pH range may be due to competitive adsorption of OH ions and dye anions. For this purpose, the further adsorption experiments are all conducted in the acidic condition.

To further confirm the adsorption mechanism of the PVA/PAA@PDA adsorbent described above, additional adsorption experiments towards different dyes has been conducted. Methyl orange and methyl violet have been selected in this part. The conditions of the experiment are exactly the same as previous and the adsorption ability of PVA/PAA@PDA membranes for different dyes is presented in Fig. 6. It can be seen that the adsorption capability of PVA/PAA@PDA toward the two dyes are lower than that of MB. According to the adsorption mechanism discussed above, the adsorption is mainly ascribed to the electrostatic interaction and hydrogen bonding between PDA layer and organic dyes, which indicates the adsorbent has better capacity for the dyes with more positive charged [41], and provide further evidence to support the above claims. Besides, it is obvious that the PVA/PAA@PDA membrane exhibits good performance on adsorbing various dyes, indicating its potential value in the removal of various dye pollutants from wastewater.

For a comparative and comprehensive study, the adsorption behavior of various PVA/PAA@PDA membranes (with different PDA loading levels) for MB and the dependence of adsorption amounts on adsorption time are presented in Fig. 7. Compared to the pure PVA/PAA membrane, PVA/PAA@PDA membranes show remarkable adsorption rate and capability towards MB. It can be seen that the PVA/PAA fiber membrane has trace adsorption amount for MB even after an equilibrium time of 75 min, whereas MB was immediately adsorbed on PVA/PAA@PDA fiber membranes within 10 min. Furthermore, the adsorption of MB almost reached an equilibrium after only 75 min with saturation adsorption amount of 314.8, 356.1, 445.7, and 296.1 mg g^{-1} for PVA/PAA@PDA-5, PVA/PAA@PDA-15, PVA/PAA@PDA-30, and PVA/PAA@PDA-45 membranes, respectively. It can be seen that the adsorption amount of MB increases with the immersion time except for PVA/PAA@PDA-45 membrane. Its low adsorption amount can be explained by the reduction of efficient active sites induced by its blocked porous structure [42], as shown in Fig. 2f. These results indicate that both the porous structure of PVA/PAA@PDA membranes and the PDA layer on the surface of fibers can be beneficial for the adsorption efficiency. Firstly, the porous structure of electrospun nanofiber membranes offers a high contact area between the adsorbent and adsorbate, which distinctly facilitates the diffusion of MB molecules. To better support the importance of the porous structure provided by electrospun membranes, the adsorption performance of pure PDA has

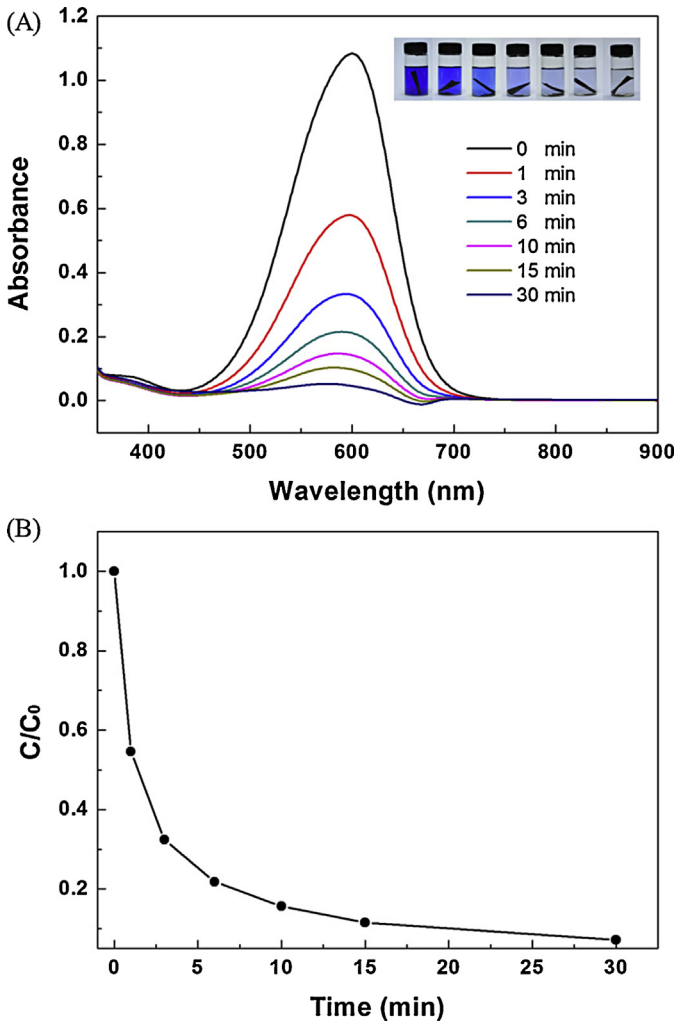

Fig. 4. UV–vis spectra of MB aqueous solution in the presence of PVA/PAA@PDA-15 membrane at time intervals of 0, 1, 3, 6, 10, 15, and 30 min, respectively. The insets are the digital photographs of MB solutions at corresponding given time intervals (A). Dependence of MB concentration on absorption time (B). MB concentration: 50 mg L^{-1}, adsorbent dosage: 10–12 mg.

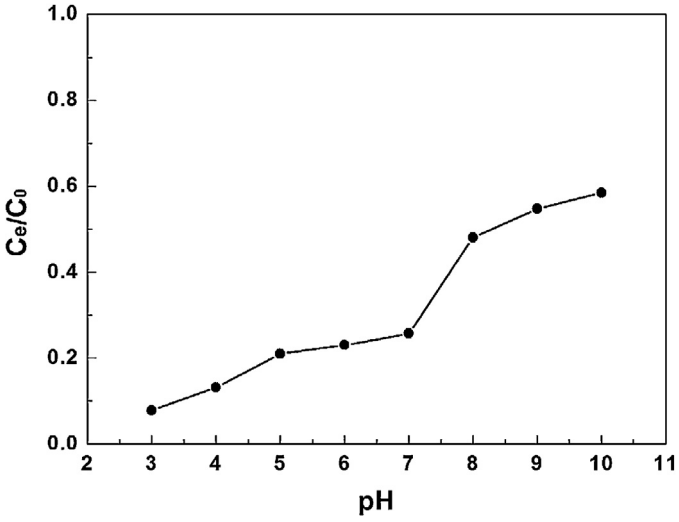

Fig. 5. Effects of pH values on the adsorption ability of PVA/PAA@PDA membranes towards methyl blue. MB concentration: 50 mg L^{-1}, adsorbent dosage: 10–12 mg.

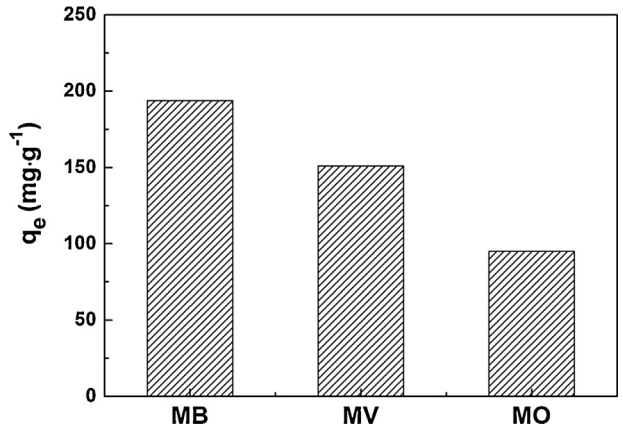

Fig. 6. Adsorption ability for various dyes at equilibrium state. Dye concentration: 50 mg L^{-1}, adsorbent dosage: 10–12 mg, pH: 3–4.

been investigated. As shown in Fig. S2, the adsorption ability of the PDA particles is much lower than that of the electrospun membranes based adsorbent. Secondly, the PDA layer coated fibrous mats act as a mimic of the mussel thread coating chemistry, providing active sites on the surface of electrospun fibers for efficient MB adsorption.

3.3. Recycle performance

When an adsorbent is used for applications, it is preferable that good recovery can be achieved by a simple procedure. Here, PVA/PAA@PDA-15 and PVA/PAA@PDA-30 membranes were selected to explore the potential reutilization for MB removal. Unlike many other nanoparticle adsorbents, the free-standing membrane adsorbents obtained in our work can be easily separated from solution. After adsorption, PVA/PAA@PDA membranes were put into NaOH solution for 10 min, followed by thoroughly washing process to remove remaining NaOH and regenerate membranes. The recycling performance of different PVA/PAA@PDA membranes is presented in Fig. 8. It can be seen that even after 10 adsorption cycles, the adsorption amount towards MB maintains at about 250 mg g^{-1} (70%, compared to 350 mg g^{-1} in the first adsorption) for PVA/PAA@PDA-15 and 300 mg g^{-1} (65%, compared to 450 m g g^{-1} in the first adsorption) for PVA/PAA@PDA-30 membranes, indicating a good recyclability of the PVA/PAA@PDA membranes. The insets of Fig. 8 show the digital photos of PVA/PAA@PDA-15 and

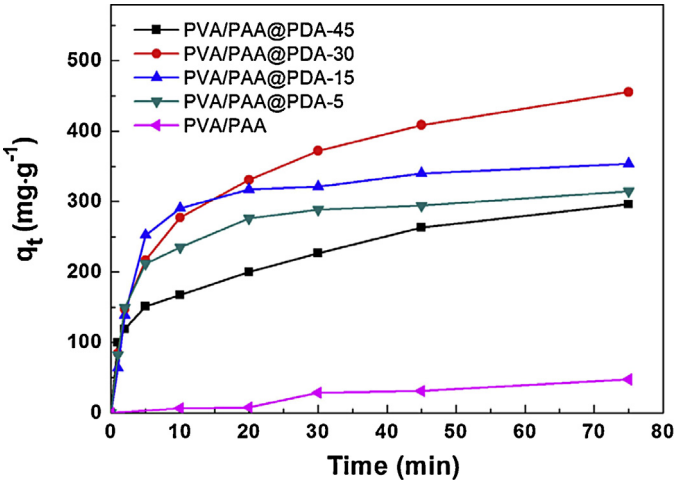

Fig. 7. MB adsorption amounts of various PVA/PAA@PDA membranes as a function of time. MB concentration: 100 mg L^{-1}, adsorbent dosage: 10–12 mg, pH: 3–4.

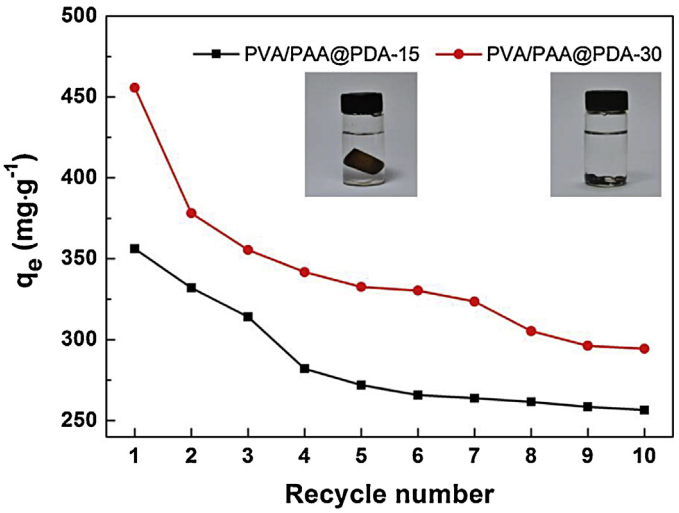

Fig. 8. Relative adsorption amount of PVA/PAA@PDA membranes towards MB at room temperature for different recycle numbers and digital photographs of the membranes after 10 adsorption–desorption cycles. MB concentration: 100 mg L^{-1}, adsorbent dosage: 10–12 mg, pH: 3–4.

PVA/PAA@PDA-30 membranes, respectively, after 10 adsorption-desorption cycles. However, it is obvious that PVA/PAA@PDA-15 membrane still keeps in one piece, while PVA/PAA@PDA-30 membrane was broken into pieces under the same operation condition, which is in accordance with the flexibility difference of the membranes as discussed above. Moreover, it is also evident that the adsorption amount of MB gradually decreases with increasing the cycle number. One possible reason can be that during adsorption–desorption cycles, the tiny wrinkles on the surface of PDA layer gradually wear off in agitated aqueous environment (Fig. S3), which directly leads to the reduction of active adsorption sites. Actually, the PDA is not as stable as expected in strong base solution [43]. In this work, the concentration of NaOH solution and the elution time have been controlled in an appropriate range, and thus the damage to the PDA layer is limited and the recycling performance of the adsorbent also provides strong evidence. At the same time, it can be seen the fibrous structure of PVA/PAA@PDA membranes is still intact even after 10 cycles, proving its good reusability in another perspective.

3.4. Adsorption kinetics

The kinetic study of the adsorption process can provide useful information regarding the adsorption efficiency and the possibility for scale-up operations. Considering the adsorption ability and recycling tests, PVA/PAA@PDA-15 membrane has been chosen to investigate the mechanism of adsorption process. Two kinetic models (the pseudo-first-order model and pseudo-second-order model), considered as the most matching models to quantify the process of uptake and study the adsorption kinetics of dyes [44,45], are used to evaluate the experimental data. The models can be expressed as follows:

Pseudo-first-order model:

$$\ln(q_e - q_t) = \ln q_e - k_1 t \quad (3)$$

Pseudo-second-order model:

$$\frac{t}{q_t} = \frac{1}{k_2 q_e^2} + \frac{t}{q_e} \quad (4)$$

where k_1 (min^{-1}) and k_2 (g mg^{-1} min^{-1}) are the rate constants of the pseudo-first-order and pseudo-second-order models, respectively. The adsorption data of PVA/PAA@PDA-15 membrane were

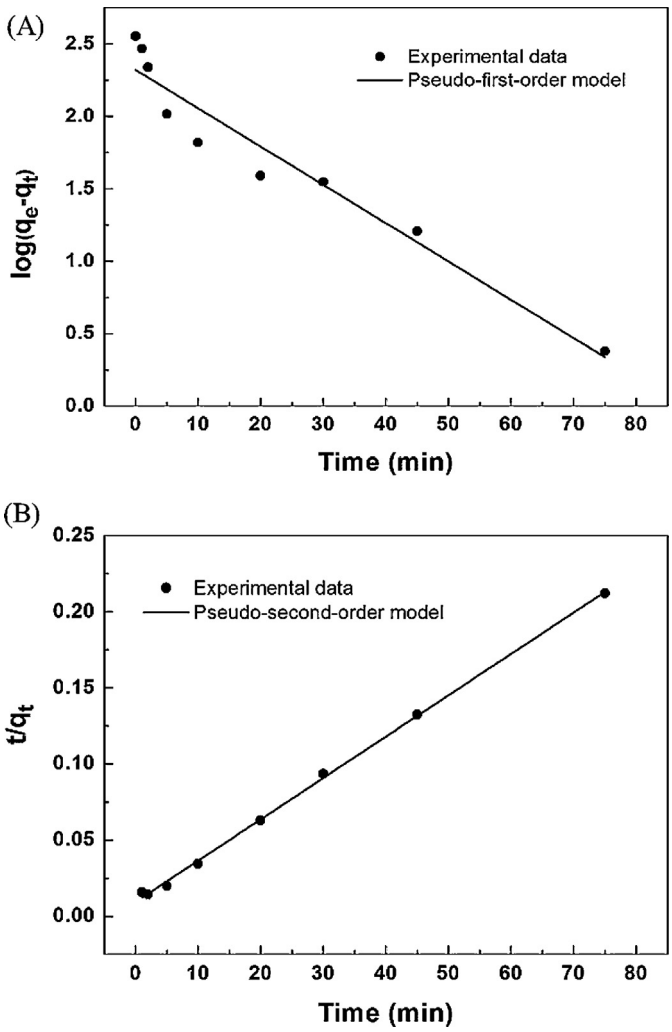

Fig. 9. Pseudo-first-order kinetic plots (A) and pseudo-second-order kinetic plots (B) for adsorption of MB on PVA/PAA@PDA-15 membrane.

Table 1
Parameters of the kinetic models fitting to the experimental data.

Model	$q_{e,\exp}$ (mg g^{-1})	$q_{e,\mathrm{cal}}$ (mg g^{-1})	k	R^2
Pseudo-first-order	356.1	10.2	0.0264	0.9331
Pseudo-second-order	356.1	369.0	0.0008	0.9988

fitted to Eqs. (3) and (4). The plots of the linearized form of kinetic models are shown in Fig. 9. The kinetic parameters and the correlation coefficients (R^2) obtained from Fig. 9 are listed in Table 1. The R^2 value of pseudo-second-order kinetic model (0.9988) is higher than that of pseudo-first-order model (0.9331). Besides, the calculated q_e value from the pseudo-second-order model fits better to the experimental data, compared to that of pseudo-first-order model. Therefore, the pseudo-second-order model is more suitable to describe the adsorption process of MB onto PVA/PAA@PDA membranes, which indicates that the chemical adsorption through sharing or exchanging electrons between adsorbent and adsorbate might be the rate-limiting step [45].

3.5. Adsorption isotherms

To further investigate the adsorption behavior of PVA/PAA@PDA membranes, two widely used isotherm equations, namely Langmuir and Freundlich isotherm model [46,47], were employed to fit the equilibrium data of MB adsorption. The Langmuir isotherm

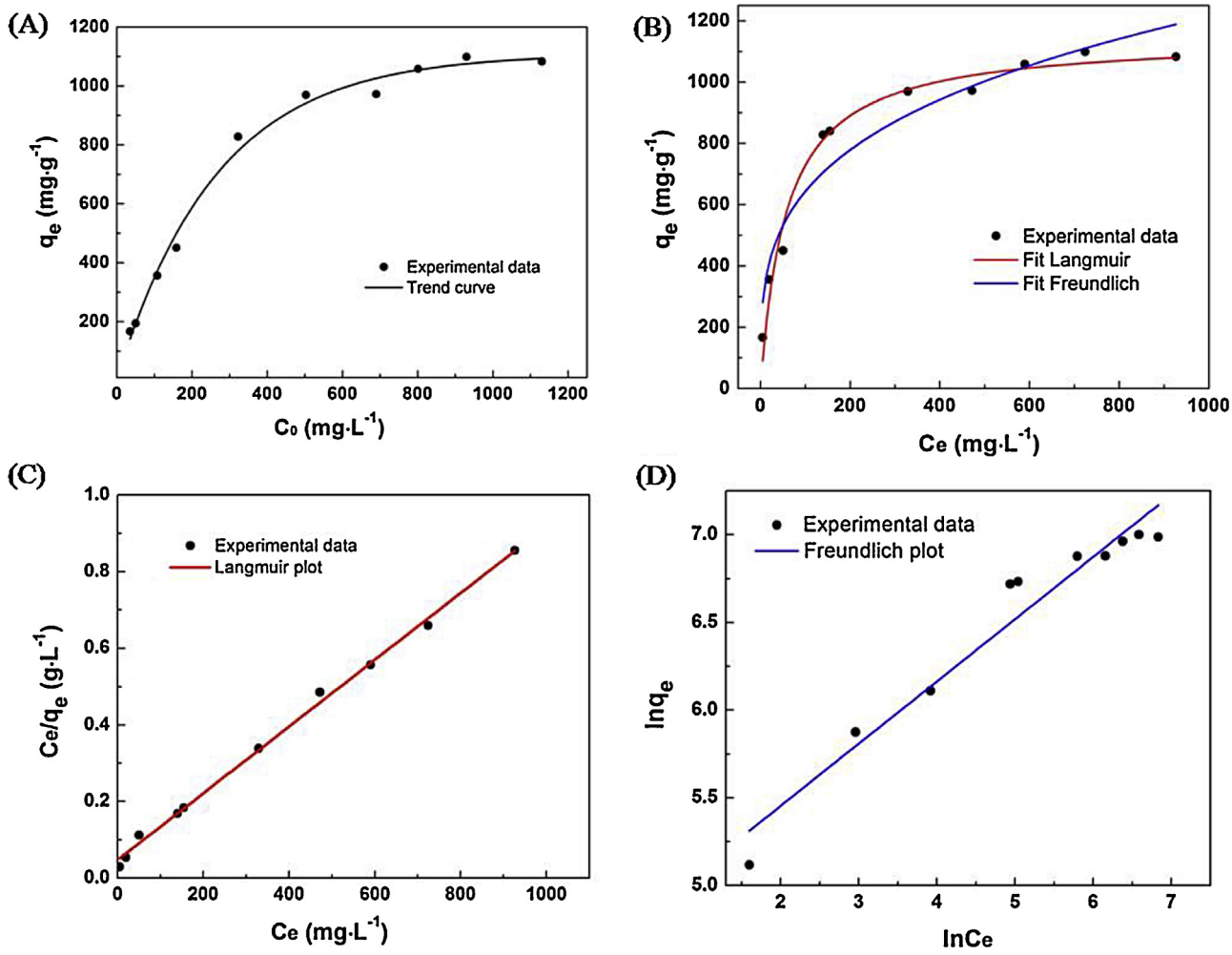

Fig. 10. Adsorption isotherms (A and B) and the corresponding Langmuir plot (C), Freundlich plot (D) for MB adsorption on PVA/PAA@PDA-15 membrane.

model is based on the assumption that the adsorption is monolayer and the adsorbent surface consists of active sites with uniform energy. In contrast, the Freundlich model assumes that the adsorbent surface is heterogeneous and the binding force decreases with the increased site occupation. The two isotherm models can be described by Eqs. (5) and (6), respectively:

Langmuir model:

$$\frac{C_e}{q_e} = \frac{(1 + C_e K_L)}{q_m K_L} \tag{5}$$

Freundlich model:

$$\ln q_e = \ln K_F + \frac{1}{n} \ln C_e \tag{6}$$

In the expressions, q_m is the calculated maximum capacity of the adsorbent. K_L is the Langmuir constant related to the adsorption rate. K_F is defined as the adsorption capacity of the adsorbent. The value of $1/n$ represents the adsorption intensity or surface heterogeneity.

The adsorption isotherms and the corresponding Langmuir plot, Freundlich plot for MB adsorption on PVA/PAA@PDA-15 membrane are presented in Fig. 10. The calculated Langmuir parameters (K_L and q_m) and Freundlich parameters (K_F and $1/n$) for the adsorption isotherms are listed in Table 2. By comparing the values of R^2, it is obvious that the adsorption data of MB is consistent with the Langmuir model, which proves that the surface of PVA/PAA@PDA-15 membrane is relatively uniform, and monolayer adsorption plays a leading role in the adsorption process. In addition, the experimental data reveal that adsorption amount of the adsorbent towards MB increases with increasing initial dye concentration. The adsorption capacity reaches up to 1147.6 mg g^{-1} according to the regression of Langmuir model, which is very prominent compared with other adsorbents reported in the literatures, as listed in Table 3. The high capacity with fast adsorption kinetics implies that PVA/PAA@PDA

Table 2
Evaluated model parameters of the adsorption isotherms for MB onto PVA/PAA@PDA-15 membrane.

Isotherms	Langmuir	Freundlich
Parameters	q_m = 1147.6 mg g^{-1} K_L = 0.0184 L mg^{-1} R^2 = 0.9966	$1/n$ = 0.3551 K_F = 114.8 mg g^{-1} R^2 = 0.9416

Table 3
Comparison of the adsorption capacity of methyl blue by different adsorbents.

Adsorbent	q_m (mg g^{-1})	References
Activated charcoal	25.3	[48]
Magnetic $Ni_{0.5}Zn_{0.5}Fe_2O_4$ nanoparticles	54.7	[49]
Magnetic chitosan grafted with graphene oxide	95.2	[50]
Organo–bentonite	98.2	[51]
$La_{1-x}K_xFeO_3$ ($x \leq 0.2$) microtubes	173.7	[52]
Poly(3-ethyl-1-vinylimidazolium bis(trifluoromethanesulfonyl) imide)	476.2	[53]
PDA assembled graphene aerogel	300	[41]
PVA/PAA@PDA membranes	1147.6	This work

membranes are highly competitive as an effective adsorbent for the removal of MB.

4. Conclusions

In summary, a novel adsorbent of PVA/PAA@PDA membranes has been developed by coating polydopamine on electrospun PVA/PAA fibers via a simple biologically inspired immersion process. Because of its porous structure and the adhesion property derived from PDA layer, PVA/PAA@PDA membranes can adsorb more than 93% of methyl blue (50 mg L^{-1}) in the solution within 30 min, indicating an efficient adsorption capability towards MB. Besides, the membrane adsorbent can be easily separated from dye solution and shows a good recycling ability. The analyses of the adsorption kinetics and isotherms indicate that the adsorption process is dominated by monolayer adsorption and chemical adsorption is the rate-limiting step. Moreover, the adsorption capacity of PVA/PAA@PDA-15 membrane towards methyl blue reaches up to 1147.6 mg g^{-1} and the general applicability in the removal of various dyes is also worth mentioning. Therefore, the PVA/PAA@PDA membrane is expected to be a very promising adsorbent for dye wastewater treatment.

Acknowledgement

The authors are grateful for the financial support from the National Natural Science Foundation of China (51373037, 51125011).

Appendix A. Supplementary data

Supplementary data associated with this article can be found, in the online version, at http://dx.doi.org/10.1016/j.jhazmat.2014.10.040.

References

[1] T. Robinson, G. McMullan, R. Marchant, P. Nigam, Remediation of dyes in textile effluent: a critical review on current treatment technologies with a proposed alternative, Bioresour. Technol. 77 (2001) 247–255.
[2] J. Szlinder-Richert, Z. Usydus, M. Malesa-Ciećwierz, L. Polak-Juszczak, W. Ruczyńska, Marine and farmed fish on the polish market: comparison of the nutritive value and human exposure to PCDD/Fs and other contaminants, Chemosphere 85 (2011) 1725–1733.
[3] G. McMullan, C. Meehan, A. Conneely, N. Kirby, T. Robinson, P. Nigam, I.M. Banat, R. Marchant, W.F. Smyth, Microbial decolourisation and degradation of textile dyes, Appl. Microbiol. Biotechnol. 56 (2001) 81–87.
[4] S. Raghu, C. Ahmed Basha, Chemical or electrochemical techniques, followed by ion exchange, for recycle of textile dye wastewater, J. Hazard. Mater. 149 (2007) 324–330.
[5] R. Hage, A. Lienke, Applications of transition-metal catalysts to textile and wood-pulp bleaching, Angew. Chem. Int. Ed. 45 (2006) 206–222.
[6] Q.W. Ding, Y.E. Miao, T.X. Liu, Morphology and photocatalytic property of hierarchical polyimide/ZnO fibers prepared via a direct ion-exchange process, ACS Appl. Mater. Interfaces 5 (2013) 5617–5622.
[7] T.C. Kim Park, S. Kim, Water recycling from desalination and purification process of reactive dye manufacturing industry by combined membrane filtration, J. Cleaner Prod. 13 (2005) 779–786.
[8] V.K. Gupta, Suhas, Application of low-cost adsorbents for dye removal – a review, J. Environ. Manage. 90 (2009) 2313–2342.
[9] M. Rafatullah, O. Sulaiman, R. Hashim, A. Ahmad, Adsorption of methylene blue on low-cost adsorbents: a review, J. Hazard. Mater. 177 (2010) 70–80.
[10] T.Y. Ren Si, J.M. Yang, B. Ding, X.X. Yang, F. Hong, J.Y. Yu, Polyacrylonitrile/polybenzoxazine-based Fe_3O_4@carbon nanofibers: hierarchical porous structure and magnetic adsorption property, J. Mater. Chem. 22 (15) (2012) 919–15927.
[11] C. Namasivayam, D. Kavitha, Removal of Congo red from water by adsorption onto activated carbon prepared from coir pith, an agricultural solid waste, Dyes Pigm. 54 (2002) 47–58.
[12] A. Gil, F.C.C. Assis, S. Albeniz, S.A. Korili, Removal of dyes from wastewaters by adsorption on pillared clays, Chem. Eng. J. 168 (2011) 1032–1040.
[13] A. Espantaleón, Use of activated clays in the removal of dyes and surfactants from tannery waste waters, Appl. Clay Sci. 24 (2003) 105–110.
[14] L.F. Vieira Ferreira, M.J. Lemos, M.J. Reis, A.M. Botelho Do Rego, UV–vis absorption, luminescence, and X-ray photoelectron spectroscopic studies of rhodamine dyes adsorbed onto different pore size silicas, Langmuir 16 (2000) 5673–5680.
[15] M.S. Chiou, H.Y. Li, Adsorption behavior of reactive dye in aqueous solution on chemical cross-linked chitosan beads, Chemosphere 50 (2003) 1095–1105.
[16] L.J. Liu Zhang, R.C. Tang, Adsorption and functional properties of natural lac dye on chitosan fiber, React. Funct. Polym. 73 (2013) 1559–1566.
[17] W.M. Zhang, C.H. Hong, B.C. Pan, Z.W. Xu, Q.J. Zhang, Q.R. Zhang, A comparative study of the adsorption properties of 1-naphthylamine by XAD-4 and NDA-150 polymer resins, Colloids Surf. A 331 (2008) 257–262.
[18] E. Yavuz, G. Bayramoğlu, M.Y. Arica, B.F. Senkal, Preparation of poly (acrylic acid) containing core-shell type resin for removal of basic dyes, J. Chem. Biotechnol. 86 (2011) 699–705.
[19] D.H. Reneker, I. Chun, Nanometre diameter fibres of polymer, produced by electrospinning, Nanotechnology 7 (1996) 216.
[20] D. Li, Y.N. Xia, Electrospinning of nanofibers: reinventing the wheel? Adv. Mater. 16 (2004) 1151–1170.
[21] J.Y. Lin, J.M. Ding, J.M. Yang, J.Y. Yu, Subtle regulation of the micro-and nanostructures of electrospun polystyrene fibers and their application in oil absorption, Nanoscale 4 (2012) 176–182.
[22] Y. Si, X.Q. Wang, Y. Li, K. Chen, J.Q. Wang, J.Y. Yu, H.J. Wang, B. Ding, Optimized colorimetric sensor strip for mercury(II) assay using hierarchical nanostructured conjugated polymers, J. Mater. Chem. A 2 (2014) 645–652.
[23] M. Bognitzki, W. Czado, T. Frese, A. Schaper, M. Hellwig, M. Steinhart, A. Greiner, Nanostructured fibers via electrospinning, Adv. Mater. 13 (2001) 70–72.
[24] Z. Huang, Y.Z. Zhang, M. Kotaki, S. Ramakrishna, A review on polymer nanofibers by electrospinning and their applications in nanocomposites, Compos. Sci. Technol. 63 (2003) 2223–2253.
[25] H.T. Zhang, H.L. Nie, D.G. Yu, C.Y. WU, Y.L. Zhang, C.J. White, L.M. Zhu, Surface modification of electrospun polyacrylonitrile nanofiber towards developing an affinity membrane for bromelain adsorption, Desalination 256 (2010) 141–147.
[26] Y.E. Miao, R.Y. Wang, D. Chen, Z.Y. Liu, C.J.B. Liu, Electrospun self-standing membrane of hierarchical SiO_2@ γ-AlOOH (Boehmite) core/sheath fibers for water remediation, ACS Appl. Mater. Interfaces 4 (2012) 5353–5359.
[27] H. Lee, S.M. Dellatore, W.M. Miller, P.B. Messersmith, Mussel-inspired surface chemistry for multifunctional coatings, Science 318 (2007) 426–430.
[28] J.H. Waite, X. Qin, Polyphosphoprotein from the adhesive pads of mytilus edulis, Biochemistry 40 (2001) 2887–2893.
[29] J.H. Ryu, Y. Lee, W.H. Kong, T.G. Kim, T.G. Park, H. Lee, Catechol-functionalized chitosan/pluronic hydrogels for tissue adhesives and hemostatic materials, Biomacromolecules 12 (2011) 2653–2659.
[30] S.L. Phua, L. Yang, C.L. Toh, S. Huang, Z. Tsakadze, S.K. Lau, Y. Mai, X. Lu, Reinforcement of polyether polyurethane with dopamine-modified clay: the role of interfacial hydrogen bonding, ACS Appl. Mater. Interfaces 4 (2012) 4571–4578.
[31] H.W. Yang, Y. Lan, W. Zhu, W.N. Li, D. Xu, J.C. Cui, D.Z. Shen, G.T. Li, Polydopamine-coated nanofibrous mats as a versatile platform for producing porous functional membranes, J. Mater. Chem. 22 (16) (2012) 994–17001.
[32] H.Y. Son, J.H. Ryu, H. Lee, Y.S. Nam, Silver-polydopamine hybrid coatings of electrospun poly(vinyl alcohol) nanofibers, Macromol. Mater. Eng. 298 (2013) 547–554.
[33] H.C. Gao, Y.M. Sun, J.J. Zhou, R. Xu, H.W. Duan, Mussel-inspired synthesis of polydopamine-functionalized graphene hydrogel as reusable adsorbents for water purification, ACS Appl. Mater. Interfaces 5 (2013) 425–432.
[34] S.X. Zhang, Y.Y. Zhang, G.M. Bi, J.S. Liu, Z.G. Wang, Q. Xu, H. Lui, X.Y. Li, Mussel-inspired polydopamine biopolymer decorated with magnetic nanoparticles for multiple pollutants removal, J. Hazard. Mater. 270 (2014) 27–34.
[35] Y. Yu, J.G. Shapter, R. Popelka-Filcoff, J.W. Bennett, A.V. Ellis, Copper removal using bio-inspired polydopamine coated natural zeolites, J. Hazard. Mater. 273 (2014) 174–182.
[36] J. Zeng, H.Q. Hou, J.H. Wendorff, A. Grenier, Electrospun poly(vinyl alcohol)/poly(acrylic acid) fibres with excellent water-stability, e-Polymer 4 (2004) 899–906.
[37] E. Baştürk, S. Demir, O. Danış, M.V. Kahraman, Covalent immobilization of ş-amylase onto thermally crosslinked electrospun PVA/PAA nanofibrous hybrid membranes, J. Appl. Polymer Sci. 127 (2013) 349–355.
[38] A. Postma, Y. Yan, Y. Wang, A.N. Zelikin, E. Tjipto, F. Caruso, Self-polymerization of dopamine as a versatile and robust technique to prepare polymer capsules, Chem. Mater. 21 (2009) 3042–3044.
[39] S.S. Chen, Y.W. Cao, J.C. Feng, Polydopamine As an efficient and robust platform to functionalize carbon fiber for high-performance polymer composites, ACS Appl. Mater. Interfaces 6 (2014) 349–356.
[40] N.G. Rim, S.J. Kim, Y.M. Shin, I. Jun, D.W. Lim, J.H. Park, H. Shin, Mussel-inspired surface modification of poly(L-lactide) electrospun fibers for modulation of osteogenic differentiation of human mesenchymal stem cells, Colloids Surf. B 91 (2012) 189–197.
[41] C. Cheng, S. Li, J. Zhao, X.X. Li, Z.Y. Liu, L. Ma, X. Zhang, S.D. Sun, C.S. Zhao, Biomimetic assembly of polydopamine-layer on graphene: mechanisms, versatile 2D and 3D architectures and pollutant disposal, Chem. Eng. J. 228 (2013) 468–481.

[42] S.J. Park, Y.S. Jang, Pore structure and surface properties of chemically modified activated carbons for adsorption mechanism and rate of Cr(VI), J. Colloid Interface Sci. 249 (2002) 458–463.
[43] S. Kim, T. Gim, S.M. Kang, Stability-enhanced polydopamine coatings on solid substrates by iron(III) coordination, Prog. Org. Coat. 77 (2014) 1336–1339.
[44] R. Jain, S. Sikarwar, Adsorptive and desorption studies on toxic dye erioglaucine over deoiled mustard, J. Dispersion Sci. Technol. 31 (2010) 883–893.
[45] Y.S. Ho, G. McKay, Pseudo-second order model for sorption processes, Process Biochem. 34 (1999) 451–465.
[46] K.Y. Foo, B.H. Hameed, Insights into the modeling of adsorption isotherm systems, Chem. Eng. J. 156 (2010) 2–10.
[47] Z. Yang, S.S. Ji, W. Gao, C. Zhang, L.L. Ren, W.W. Tjiu, Z. Zhang, J.S. Pan, T.X. Liu, Magnetic nanomaterial derived from graphene oxide/layered double hydroxide hybrid for efficient removal of methyl orange from aqueous solution, J. Colloid Interface Sci. 408 (2013) 25–32.
[48] M.J. Iqbal, M.N. Ashiq, Adsorption of dyes from aqueous solutions on activated charcoal, J. Hazard. Mater. 139 (2007) 57–66.
[49] R.J. Liu, X.Q. Shen, X.C. Yang, Q.J. Wang, F. Yang, Adsorption characteristics of methyl blue onto magnetic $Ni_{0.5}Zn_{0.5}Fe_2O_4$ nanoparticles prepared by the rapid combustion process, J. Nanopart. Res. 15 (2013) 1679.
[50] L.L. Fan, C.N. Luo, X.J. Li, F.G. Lu, H.M. Qiu, M. Sun, Fabrication of novel magnetic chitosan grafted with graphene oxide to enhance adsorption properties for methyl blue, J. Hazard. Mater. 215 (2012) 272–279.
[51] X.L. Hao, H. Liu, G.S. Zhang, H. Zou, Y.B. Zang, M.M. Zhou, Y.C. Gu, Magnetic field assisted adsorption of methyl blue onto organo-bentonite, Appl. Clay Sci. 55 (2012) 177–180.
[52] L.L. Zou, R.J. Liu, X.Q. Shen, Q.J. Wang, H.Q. Feng, Preparation of $La_{1-x}K_xFeO_3$ microtubes and their adsorption kinetics of methyl blue, J. Nanosci. Nanotechnol. 14 (2014) 2919–2924.
[53] H. Mi, Z.G. Jiang, J. Kong, Hydrophobic poly(ionic liquid) for highly effective separation of methyl blue and chromium ions from water, Polymers 5 (2013) 1203–1214.